Cerebral Cortex, 2017; 1–14

doi: 10.1093/cercor/bhx325
Original Article

ORIGINAL ARTICLE

The Ventral Posterior Lateral Thalamus Preferentially Encodes Externally Applied Versus Active Movement: Implications for Self-Motion Perception

Alexis Dale and Kathleen E. Cullen

Department of Physiology, McGill University, Montreal, Quebec, Canada H3G 1Y6

Address correspondence to Kathleen E. Cullen, McIntyre Medical Building, Room 1219, 3655 Promenade Sir William Osler, Montreal, Quebec, Canada H3G 1Y6. Email: kathleen.cullen@mcgill.ca

Abstract

Successful interaction with our environment requires that voluntary behaviors be precisely coordinated with our perception of self-motion. The vestibular sensors in the inner ear detect self-motion and in turn send projections via the vestibular nuclei to multiple cortical areas through 2 principal thalamocortical pathways, 1 anterior and 1 posterior. While the anterior pathway has been extensively studied, the role of the posterior pathway is not well understood. Accordingly, here we recorded responses from individual neurons in the ventral posterior lateral thalamus of macaque monkeys during externally applied (passive) and actively generated self-motion. The sensory responses of neurons that robustly encoded passive rotations and translations were canceled during comparable voluntary movement (~80% reduction). Moreover, when both passive and active self-motion were experienced simultaneously, neurons selectively encoded the detailed time course of the passive component. To examine the mechanism underlying the selective elimination of vestibular sensitivity to active motion, we experimentally controlled correspondence between intended and actual head movement. We found that suppression only occurred if the actual sensory consequences of motion matched the motor-based expectation. Together, our findings demonstrate that the posterior thalamocortical vestibular pathway selectively encodes unexpected motion, thereby providing a neural correlate for ensuring perceptual stability during active versus externally generated motion.

Key words: corollary discharge, efference copy, exafference, reafference, rhesus monkey

Introduction

The thalamus is commonly considered to be the primary relay of sensory information to the cortex. In the vestibular system, there are 2 main thalamocortical pathways—1 anterior and 1 posterior—that transmit self-motion information to regions of the cortex mediating high-level functions such as the computation of spatial orientation and perception of self-motion (Shinder and Taube 2010; Hitier et al. 2014; Wijesinghe et al. 2015). The circuit targeted by the anterior pathway includes the anterior dorsal thalamus, the entorhinal cortex and presubiculum, and the retrosplenial cortex—all part of the head direction (HD) cell network (reviewed in Taube 2007). Importantly, this pathway has been linked to navigation and spatial memory in freely moving rodents (Moser et al. 2008; Dumont and Taube 2015). Neurons that appear to resemble HD cells have also been recorded in the primate anterior thalamus and presubiculum (Robertson et al. 1999; Laurens et al. 2016).

In contrast, the posterior vestibulo-thalamocortical pathway (Deecke et al. 1977, Büttner and Lang 1979) has been less extensively studied despite its likely contribution to ensuring the accurate coordination of perception and action (reviewed in: Clark and Harvey 2016). To date, studies in macaques have established that neurons in the posterior thalamus, as well as their cortical targets such as parietoinsular vestibular cortex (Grüsser et al. 1990a), respond to passively applied vestibular stimulation (Meng et al. 2007; Chen et al. 2010; Meng and Angelaki 2010).

Vestibular responses to passive stimulation have also been documented in other cortical areas (area 2 v: Büttner and Buettner 1978; medial superior temporal cortex: Sakata et al. 1994, Duffy 1998; ventral intraparietal cortex: Bremmer et al. 2002). Understanding how higher-order cortical areas process sensory information to precisely coordinate our actions with our perception of self-motion, however, requires recording neuronal responses under natural conditions in which movements are typically actively generated rather than externally applied. Yet the question of how macaque thalamocortical neurons respond when vestibular stimulation is the result of self-generated motion remains open.

Here, we report on the responses of 42 individual vestibular-sensitive neurons in the ventral posterior lateral (VPL) thalamus during active and passive self-motion with matching trajectories. Each neuron's response was measured in both conditions as well as during concurrent passive and active self-motion. We find that neurons selectively encode the detailed time course of passive movements, while neuronal sensitivities to actively generated movements are significantly reduced. Moreover, when passive and active movements are experienced simultaneously, individual neurons preferentially encode the detailed time course of the passive component. We then examine the mechanism that underlies the selective elimination of vestibular sensitivity to active motion by testing 2 hypotheses. First, we ask whether nonlinear combination of vestibular and proprioceptive inputs results in reduced vestibular sensitivities. Second, we test whether a direct signal from motor pathways (e.g., an efference copy; von Holst and Mittelstaedt 1950) produces responses consistent with a cancellation signal. The results show that suppression of responses to actively generated vestibular stimulation occurs in conditions where there is a match between the sensory consequences of motion and the motor-based expectation. This suggests a role for the VPL thalamus in generating perceptually stable representations of motion via the preferential transmission of externally applied vestibular information to cortex.

Materials and Methods

All experimental procedures were approved by the McGill University Animal Care Committee, and were in compliance with the guidelines of the Canadian Council on Animal Care.

Surgical Procedures

Two male rhesus monkeys (*Macaca mulatta*) were prepared for acute extracellular recordings using aseptic surgical techniques as detailed in Dale and Cullen (Dale and Cullen 2013). Specifically, surgical levels of isoflurane (0.8–1.5%) were maintained while monkeys were implanted with a stainless steel head post for head restraint, and a recording chamber. The chamber was oriented at a 6° lateral angle and positioned over the posterior and lateral portion of the thalamus to provide access to the VPL. The implant was chronically fastened to the skull with stainless steel screws and dental acrylic. An 18 mm eye coil (3 loops of Teflon-insulated stainless steel wire) was also implanted behind the conjunctiva of one eye in each monkey (Fuchs and Robinson 1966). Finally, buprenorphine (0.01 mg/kg, IM) and cefazolin (25 mg/kg) were administered as postoperative analgesia and antibiotic, respectively. Animals recovered for at least 2 weeks before recordings began.

Data Acquisition

Throughout recordings, monkeys were seated in a dark room in a primate chair surrounded by a plain white cylindrical screen located ~60 cm from the center of the monkey's head. The chair was fixed to a linear sled that was mounted on a vestibular turntable driven by a servomotor (S72402; Kollmorgen, Radford, VA), thereby allowing both whole-body translations in any direction in the horizontal plane as well as whole-body yaw rotations. In addition, the monkey's head restraint was coupled to a head-fixed sled. A translational brake could be applied to restrict motion to head-on-body rotations in the yaw axis, and a rotational brake could be applied to restrict motion to small (±5 cm), linear head-on-body movements in either the fore-aft or lateral (interaural) directions.

Gaze and head position were measured using the magnetic search coil technique (Fuchs and Robinson 1966; Judge et al. 1980). Turntable velocity was controlled by REX, a QNX based, real-time data acquisition system (Hayes et al. 1982), and measured using an angular rate sensor (Watson Industries, Inc., Eau Claire, WI). Angular velocity and linear acceleration of the monkey's head was recorded with a microelectromechanical systems (MEMS) device, which comprised gyroscopes for 3 axes of rotation (QGYR330H; Qualtré, Inc., Marlborough, MA) and a 3D linear accelerometer (ADXL330; Analog Devices, Norwood, MA). In the head-fixed condition, the neck torque produced by the monkey against its head-restraint was measured using a reaction torque transducer (QWFK-8M; Honeywell, Canton, MA). All behavioral signals were low-pass filtered at 250 Hz, and acquired at 1 kHz sampling frequency.

The VPL was located relative to the lateral geniculate nucleus, which was recognizable due to the presence of individual neurons that responded to either the onset or offset of a light flashed while lowering the electrode during early recordings (Marrocco 1976). Each neuron included in the present report demonstrated robust firing rate modulation during sinusoidal, whole-body rotations, and insensitivity to eye movements during saccades or smooth pursuit (Roy and Cullen 2001; Marlinski and McCrea 2008a). Further, we ensured that neurons did not respond to visual stimulation caused by small spots of light presented in the visual field (Marrocco 1976). Extracellular single-unit activity was recorded using enamel-insulated tungsten microelectrodes (2–10 Mohm impedance, Frederick Haer), band-pass filtered from 300 Hz to 3 kHz, and sampled at 30 kHz. Both neural and behavioral data were acquired through the Cerebus Neural Signal Processor (Blackrock Microsystems, Salt Lake City, UT).

Passive Rotation Paradigms

Passive Vestibular Stimulation

Neurons were initially identified on the basis of their response to passive rotations in the dark in the absence of visual or proprioceptive inputs (i.e., whole-body rotations). The same stimuli were then applied with the lights on to confirm that there was no change in mean firing rate or sensitivity due to responses to visual stimulation.

Passive Neck Proprioceptive Stimulation

To characterize VPL neuronal responses to activation of neck proprioceptors in the absence of vestibular stimulation, neuronal responses were quantified during rotations when the monkey's head was held fixed in space and its body was rotated on the turntable below (i.e., body-under-head rotations).

Combined Passive Vestibular and Neck Proprioceptive Stimulation

To activate both vestibular and neck proprioceptive sensors simultaneously, the translational brake was applied and the monkey's head was passively rotated independently while its body remained stationary (i.e., passive head-on-body rotations).

Because VPL neurons have been reported to display a large decrease in sensitivity with increasing peak velocity of movement (squirrel monkey: Marlinski and McCrea 2008a), vestibular rotational sensitivities in all 3 of the above conditions were quantified for 2 types of passive motion: (1) slow, sinusoidal yaw rotations at 0.5 Hz and 1 Hz (peak velocity 40 °/s), and (2) faster rotations with a more natural trajectory that were generated from an average of the monkey's typical voluntary 60° eye-head gaze shift ("active-like" rotations, peak velocity ~180 °/s). Monkeys were well adapted to each movement condition, and quantification excluded any occasional periods when the animal attempted any intervening head or body movements.

Active Rotation Paradigms

To enable recording during voluntary movements, the monkey's head was carefully released while maintaining isolation of the neuron. Dim lights were illuminated while monkeys performed slow voluntary gaze pursuit by following a small smoothly moving target (0.5 or 1 Hz, peak velocity 40 °/s), or made voluntary gaze shifts (peak velocities 165–195 °/s) to fruit rewards alternately presented at approximately ±30° to the left and right (active head-on-body rotations). To test neuronal responses to voluntary movements in the presence of passive vestibular stimulation, concurrent passive and active rotations were achieved by applying 1 Hz passive whole-body rotations while monkeys performed active head-on-body gaze shifts.

Finally, to test the influence of motor related signals on VPL neurons, responses were recorded while monkeys made voluntary gaze shifts between food targets when their heads were unexpectedly restrained. The neck torques produced in this head-fixed condition (>1 N m) were comparable to those generated by the monkey during the gaze shift head movements described above, confirming that monkeys generated a motor command to move the head (Cullen and Roy 2004).

Translation Paradigms

Passive Translations

To test neuronal sensitivities to linear motion, sinusoidal, whole-body translations were delivered on the linear sled in both the fore-aft and lateral (interaural) directions (1 Hz, peak acceleration 0.2 *g*). If a neuron responded to whole-body translations along either axis, the translational brake on the head restraint was released and neuronal responses were also recorded to translations during which the head was moved along the head-fixed sled while the body remained stationary (head-on-body translations). Slow sinusoidal translations matching those described above, as well as active-like motion profiles matching those described below, were applied.

Active Translations

Finally, while maintaining isolation of the neuron, the monkey's head was gently released to allow voluntary movement along either the fore-aft or lateral axis of the head-fixed sled for juice reward.

Data Analysis

Neural data was imported into Offline Sorter (Plexon, Inc., Dallas, TX) to detect and mark action potentials from the isolated neuron (Dale and Cullen 2015). Briefly, action potential voltage waveforms were snipped according to a manually selected threshold crossing and aligned on their peak or trough. Time stamps assigned to each action potential were then used to generate a binary vector (1 kHz) of unit activity with 1 representing a spike and 0 representing no spike.

Behavioral data and neural time stamps were imported into the Matlab (The Mathworks, Natick, MA) programming environment for analysis. Behavioral signals were digitally low-pass filtered at 125 Hz using a 51st-order finite impulse response filter with a Hamming window, and horizontal and vertical eye positions were obtained as the difference between gaze and head position along each respective axis. Position signals were then digitally differentiated into velocity signals. Neuronal firing rate was computed by filtering spike trains with a Kaiser window (Cherif et al. 2008) 1 Hz above double the frequency of ongoing head movements. Neuronal sensitivities to vestibular and neck proprioceptive stimulation during rotations were computed using a least-squares regression analysis as described in Brooks and Cullen (2009):

$$\widehat{fr}(t) = b + g_v\omega(t) + g_a\dot{\omega}(t) \quad (1)$$

where $\widehat{fr}(t)$ is the estimated firing rate, b is a bias term, g_v and g_a are the gains (sensitivities) with respect to angular velocity, $\omega(t)$, and angular acceleration, $\dot{\omega}(t)$, respectively, either of the head (vestibular stimulation: whole-body and head-on-body rotations) or the turntable (neck proprioceptive stimulation: body-under-head rotations). Neurons with increased firing rate during ipsilateral rotations (29/42, 69%) were termed type I, while neurons with increased firing rate during contralateral rotations (13/42, 31%) were termed type II (Duensing and Schaefer 1958). Because neuronal dynamics were otherwise comparable, both types of neurons were grouped together for the analyses in this study.

Neuronal sensitivities to vestibular stimulation during translations were computed as described in Carriot et al. (2013):

$$\widehat{fr}(t) = b + g_{vt}\dot{H}(t) + g_{at}\ddot{H}(t) \quad (2)$$

where g_{vt} and g_{at} are the gains with respect to linear head velocity ($\dot{H}$) and linear acceleration ($\ddot{H}$), respectively.

Goodness-of-fit was measured by computing the variance accounted for:

$$VAF = 1 - [var(\widehat{fr}-FR) / var(FR)] \quad (3)$$

where FR is the recorded firing rate. Optimal g_v and g_a were then used to compute each neuron's sensitivity and phase shift relative to rotational velocity (Sadeghi et al. 2009):

$$S_{vel} = \sqrt{\left[g_v^2 + (2\pi f g_a)^2\right]} \quad (4)$$

$$\varphi = \left[atan\left(\frac{2\pi f g_a}{g_v}\right) - \frac{\pi}{2}\right] * \frac{180}{\pi} \quad (5)$$

and optimal g_{vt} and g_{at} were used to compute each neuron's sensitivity and phase shift relative to or linear acceleration (Carriot et al. 2015):

$$S_{accel} = \sqrt{\left[g_{at}^2 + \left(\frac{g_{vt}}{2\pi f}\right)^2\right]} \quad (6)$$

$$\varphi_t = \left[atan\left(\frac{2\pi f g_{at}}{g_{vt}}\right) - \frac{\pi}{2}\right] * \frac{180}{\pi} \quad (7)$$

In turn, S_{vel} and φ corresponding to rotations were represented as polar vectors which were used to compute population vectors representing neurons' responses to whole-body rotation (vestibular sensitivity) and body-under-head rotation (neck proprioceptive sensitivity), where the direction of body-under-head rotation was defined as opposite that of the head on the body. In addition, S_{accel} and φ_t corresponding to translations in both the fore-aft and lateral directions were used to compute the axis of maximal sensitivity for each neuron (Carriot et al. 2013). Sensitivities reported for passive and active translations were computed based on the axis (fore-aft or lateral) in which neurons responded most strongly during passive, whole-body translations. Rotational sensitivities to whole-body rotations were greater than 0.1 (spk/s)/(°/s), and translational sensitivities were greater than 50 (spk/s)/g for at least one direction of whole-body motion.

Statistical significance was computed using paired t-tests comparing neuronal responses across conditions. Unless otherwise noted, averages are reported as mean ± standard deviation.

Results

VPL Neurons: Responses to Vestibular and Neck Proprioceptive Stimulation

We recorded from 42 neurons (21 from monkey S and 21 from monkey D) in the rhesus monkey VPL thalamus that were responsive to sinusoidal whole-body yaw rotations and did not respond to horizontal or vertical eye movements, movement of small objects in the environment, or onset/offset of lights in the room (see Materials and Methods). We further characterized neurons based on their firing rate modulation during passive neck proprioceptive stimulation (i.e., body-under-head rotations; see Materials and Methods).

Figure 1 shows average responses from 2 representative neurons and the corresponding best fits (eq. 1, blue curves) in each of 3 passive stimulation conditions: vestibular stimulation alone (left panel), neck proprioceptive stimulation alone (center panel), and combined vestibular and neck proprioceptive stimulation (right panel). Notably, neurons were grouped into 2 populations. Approximately 40% of our sample (n = 17 neurons; 7 from monkey D and 10 from monkey S) resembled the top row of firing rates and did not exhibit sensitivity to neck proprioception (termed vestibular-only [VO] neurons; average vestibular sensitivity 0.63 ± 0.38 [spk/s]/[°/s]). In contrast, approximately 60% of our sample (n = 25 neurons; 14 from monkey D and 11 from monkey S) resembled the bottom row of firing rates, exhibiting both vestibular and neck proprioception responses (termed V + N neurons; average vestibular sensitivity 0.49 ± 0.17 [spk/s]/[°/s], average neck proprioceptive sensitivity 0.36 ± 0.15 [spk/s]/[°/s]).

VPL Neurons Differentiate Active From Passive Rotations

During everyday life, vestibular and proprioceptive stimulation are most often the consequence of our own actions rather than motion produced by external events. To test the hypothesis that VPL neurons differentially encode passive and active motion, we next compared neuronal responses to passively applied and self-produced (i.e., active) stimuli with similar profiles. As shown in Figure 2A, the representative VO (top panel) and V + N (bottom panel) neurons responded differently during active versus passive head movements, even though head and neck motion was comparable in both conditions. The left side of Figure 2A depicts the average firing rate modulation and corresponding best fit (blue curves) for both example neurons to repeated passive stimuli with a velocity profile designed to mimic those produced during active movements (i.e., "active-like" motion profiles; see Materials and Methods). On average, the populations of VO and V + N neurons had passive sensitivities of 0.26 ± 0.21 (spk/s)/(°/s) (range: 0.14–0.85) and 0.27 ± 0.14 (spk/s)/(°/s) (range: 0.11–0.64), respectively.

The right side of Figure 2A shows the striking difference during comparable active rotations (red curves): each neuron's response was greatly reduced, such that their firing rates did not change significantly from baseline. Indeed, predicted responses based on neuronal sensitivities to passive motion (dotted red traces) overestimated the modulation represented by the best fits (solid red curves) for both example neurons. Overall, the response sensitivities for our populations of VO and V + N neurons to active motion were reduced 83 ± 15% (n = 14 VO, P = 0.001, paired t-test) and 74 ± 19% (n = 22 V + N, $P < 10^{-6}$, paired t-test), respectively, from those to passive motion (Fig. 2B). Thus, VPL neurons do not consistently encode vestibular sensory information in all behavioral conditions, but preferentially encode externally applied motion.

Selective Encoding of Passive Motion During Active Motion

We next addressed whether VPL neurons continue to selectively encode externally applied motion when it is experienced concurrently with self-generated motion, or instead respond to total head-in-space velocity (i.e., comprising both actively and passively generated components). To distinguish between these 2 proposals, we applied passive, whole-body rotations while monkeys generated head-on-body gaze shifts, and computed neuronal sensitivities to head-in-space (i.e., total) velocity as well as to only passive velocity. As is shown for the example VO neuron in Figure 3A, instead of encoding total head-in-space velocity, the neuron continued to respond selectively to passive head motion when experienced concurrently with active motion. Specifically, whenever an active head movement was produced, the neuron's firing rate modulation was overestimated by a prediction based on its sensitivity to total head-in-space velocity during passive stimulation (i.e., Fig. 2; black curves; see Materials and Methods). In contrast, the neuron's response corresponded well to a prediction based on its sensitivity to the passive component of the motion (blue curves).

Figure 3B, C summarizes these results for our population of VO neurons (filled symbols). Neuronal sensitivities to the passive component of motion [0.39 ± 0.16 (spk/s)/(°/s)] matched those quantified for responses recorded when passive whole-body rotations were applied alone (0.35 ± 0.12 [spk/s]/[°/s]; n = 14, P = 0.06, paired t-test; Fig. 3B). In addition, consistent with the results in Figure 2, neuronal responses to the active component of concurrent motion were minimal (average sensitivity 0.02 ± 0.02 [spk/s]/[°/s]; n = 14, $P < 10^{-5}$, paired t-test; Fig. 3C). Similar results were found for our V + N neuron population

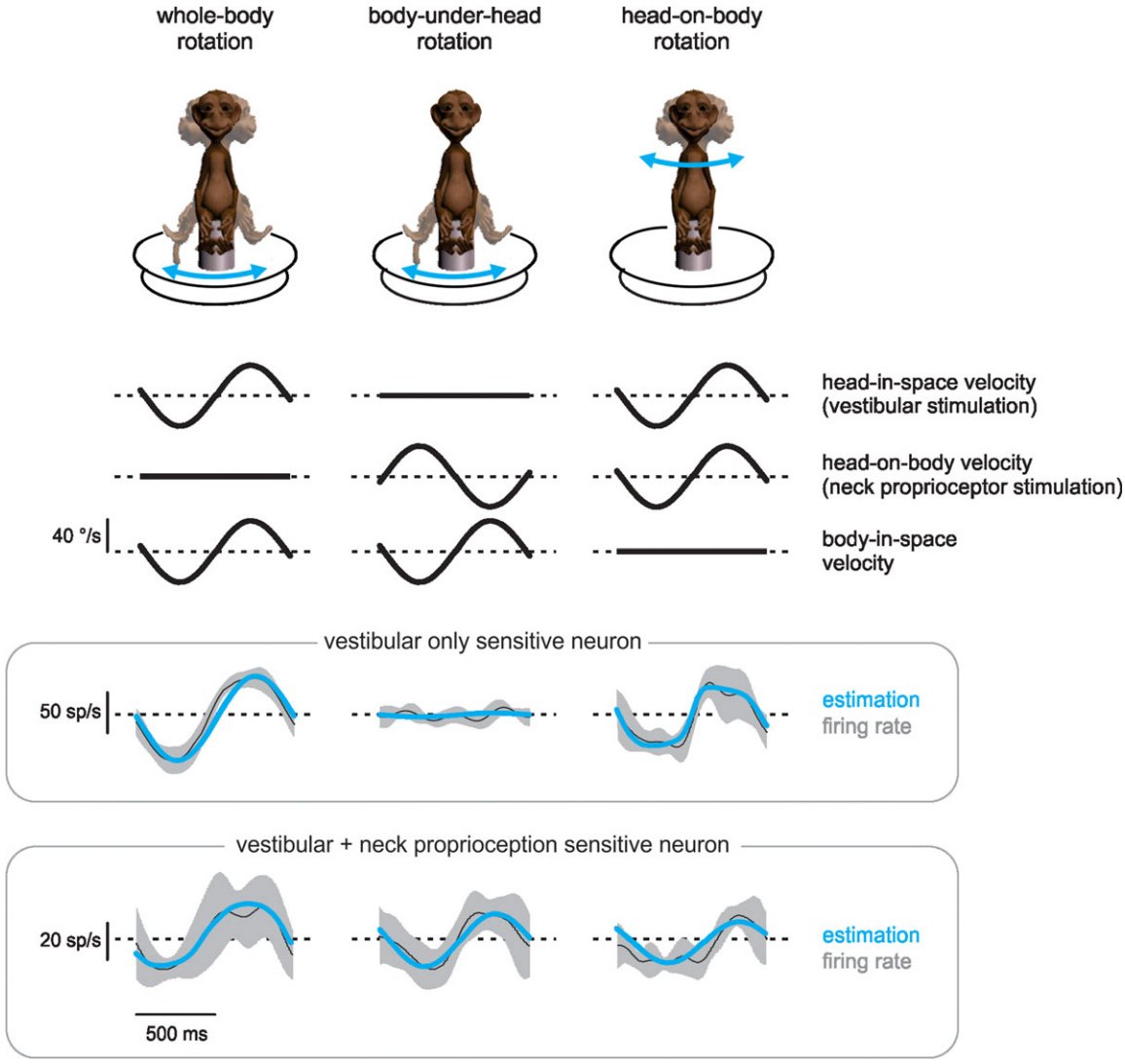

Figure 1. VPL has 2 populations of noneye movement sensitive neurons. Comparison of responses from an example vestibular-only (VO) neuron (top panel of firing rates) and an example neuron with vestibular and neck proprioception sensitivity (V + N; bottom panel of firing rates) to vestibular stimulation applied in isolation via whole-body rotations (left), neck proprioceptive stimulation applied in isolation via body-under-head rotations (center), or their combination, head-on-body rotations (right). Velocity traces are schematic representations of each condition, firing rates are averages across 10 cycles of rotation with shaded areas representing standard deviation, and estimations (blue curves) are fits to eq. 1 (see Materials and Methods). Conventions: Upward is ipsilateral for all movement traces, and superimposed dashed lines represent 0 °/s. Light dashed lines superposed on unit firing rate traces represent the mean response.

(open symbols), which are superimposed for comparison on the plots in Figure 3B ($n = 6$, $P = 0.22$, unpaired t-test) and 3C ($n = 6$, $P = 0.002$, unpaired t-test). Taken together, the results above demonstrate that vestibular-sensitive neurons in VPL differentiate active from passive self-motion via significantly attenuated responses to the self-generated component of ongoing movement, even when these actively generated signals are experienced concurrently with externally applied ones.

VPL Neurons Linearly Combine Sensitivities to Vestibular and Neck Proprioceptive Inputs During Passive but not Active Motion

In order to understand the mechanism that underlies the selective elimination of vestibular sensitivity to active head-on-body rotations, we specifically investigated neurons' responses to the simultaneous activation of both vestibular and neck proprioceptive systems, which occurs during active head-on-body rotations. Could this integration explain, at least in part, the observed attenuation of sensory responses during active head movements? We quantified each neuron's response to a series of passive stimuli that mimicked the velocity profiles of active movements and stimulated first the vestibular system alone, then the proprioceptive system alone, and finally the 2 systems together. Across our population, VO neurons responded robustly to active-like passive vestibular stimulation alone (i.e., whole-body rotations, see Materials and Methods; average sensitivity 0.32 ± 0.19 [spk/s]/[°/s]). Figure 4A plots the response vectors representing each neuron's vestibular sensitivity and modulation phase in this condition (purple arrows). In contrast, consistent with the results presented above in Figure 1 for sinusoidal stimulation, VO neurons did not respond to active-like passive stimulation of neck proprioceptors alone (i.e., body-under-head rotations; see Materials

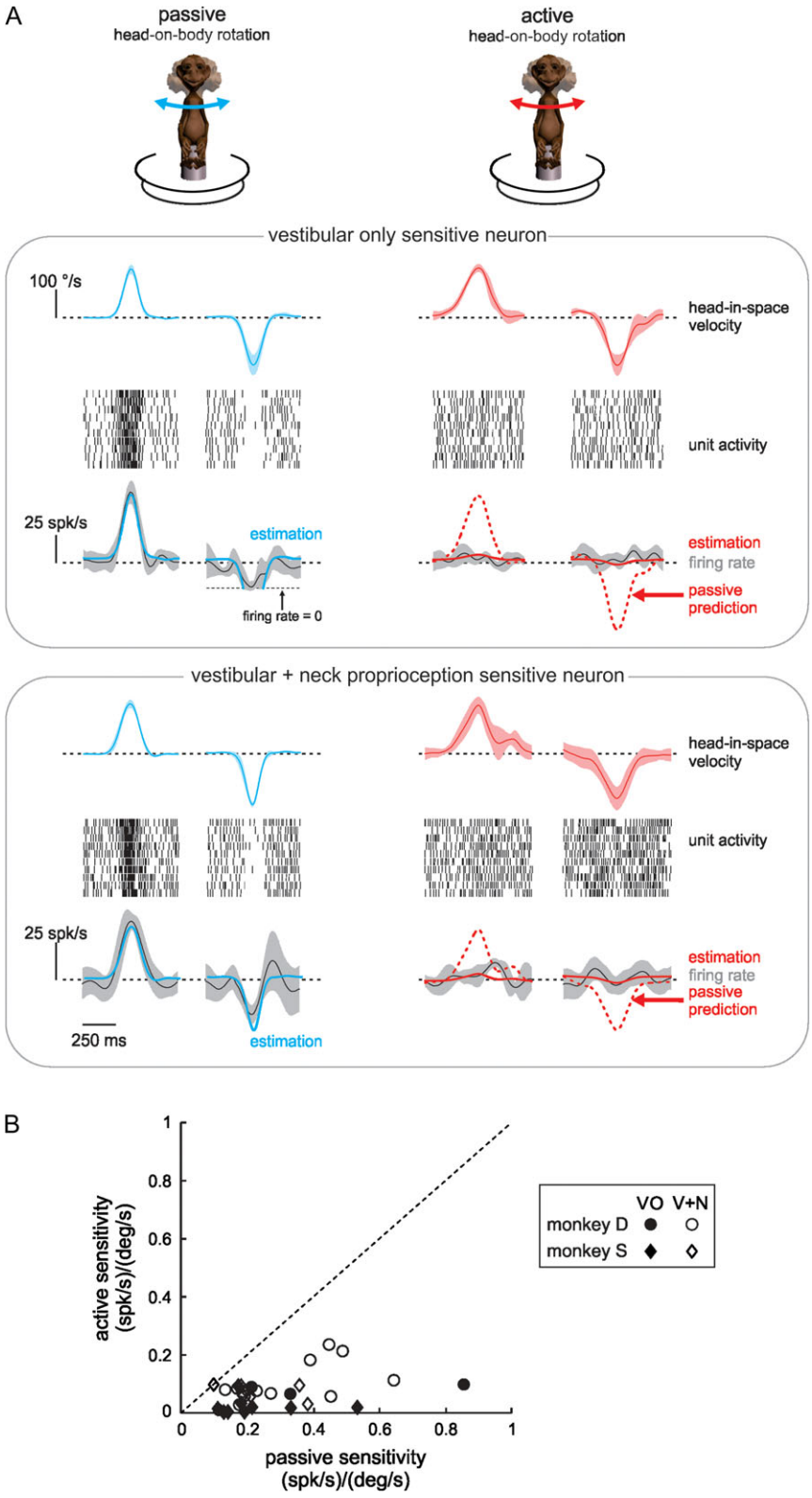

Figure 2. Thalamic inputs to cortex respond to active-like passive, but not to active rotations. (*A*) Responses of the same 2 example neurons as in Figure 1 to passively applied (blue curves) and self-generated (red curves) head-on-body rotations with comparable trajectories. Head-in-space velocity and firing rate traces are averages over 10 movements with shaded areas representing standard deviation. Conventions as in Figure 1. Raster plots show movement-by-movement spiking activity for each of the same 10 movements. Firing rate estimations (solid blue and red curves) are plotted with the same conventions as in Figure 1, and passive predictions (dashed red curves) are based on sensitivity computed from the passive estimation. (*B*) Population summaries revealing that all neurons had reduced sensitivity in response to active relative to passive rotations. Black symbols correspond to VO neurons ($n = 14$, $P = 0.001$, paired *t*-test), white symbols correspond to V + N neurons ($n = 22$, $P < 10^{-6}$, paired *t*-test), and circles versus diamonds correspond to neurons from monkeys D and S, respectively. Dotted line represents unity.

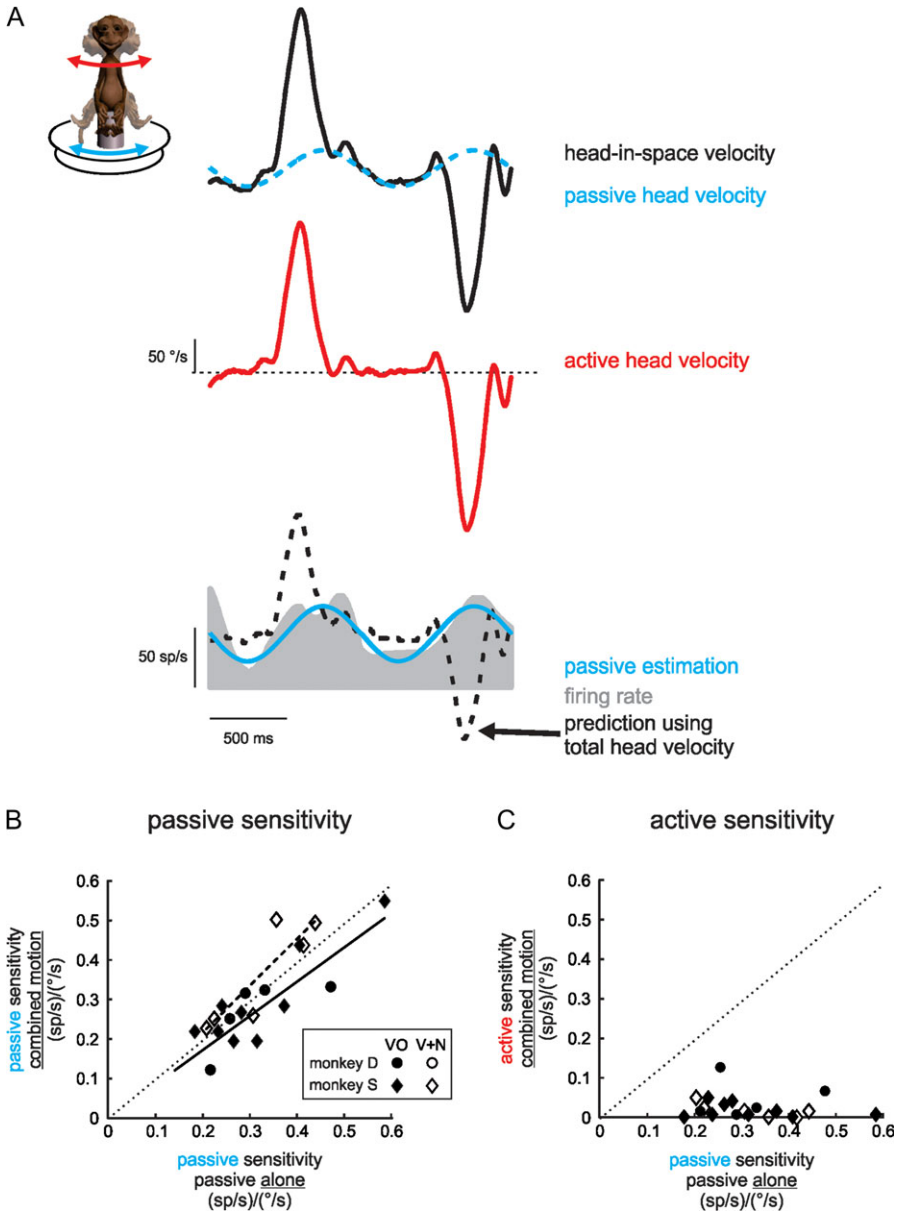

Figure 3. Neurons selectively encode the passive component of concurrent passive and active rotations. (*A*) The activity of an example VO neuron (gray trace) in response to self-generated head-on-body rotations (red curve) during simultaneous passive, whole-body rotations (dashed blue curve) is well fit by the passive component of the motion alone (solid blue curve) and is not well predicted by a response to total head-in-space velocity (black curves). Movement traces are plotted with the same conventions as in Figure 1. (*B*) For VO (black symbols, solid line [$n = 14$, $P = 0.43$, unpaired *t*-test comparison with unity]) as well as V + N neurons (white symbols, dashed line [$n = 6$, $P = 0.54$, unpaired *t*-test comparison with unity]), sensitivities to passive whole-body rotation applied concurrently with active movements were closely matched to those when the same passive motion was applied alone ($n = 14$ VO, $P = 0.06$, $n = 6$ V + N, $P = 0.22$, paired *t*-tests between passive sensitivities). (*C*) All neuronal sensitivities to active movements occurring during passive whole-body rotations were significantly reduced ($n = 14$ VO $P < 10^{-5}$, $n = 6$ V + N, $P = 0.002$, paired *t*-tests between active and passive sensitivities). Circles versus diamonds correspond to neurons recorded from monkeys D and S, respectively, and dotted lines represent unity.

and Methods). Finally, we then quantified each neuron's response when the vestibular and proprioceptive systems were passively activated together (i.e., head-on-body rotations; see Materials and Methods). Neuronal sensitivities were comparable to those observed in response to vestibular stimulation alone (0.26 ± 0.21 [spk/s]/[°/s]; $n = 12$, $P = 0.97$, paired *t*-test, compare blue and purple arrows in the inset of Fig. 4A), and were significantly larger than those observed for active movements (Fig. 4A, red arrows; $n = 12$, $P = 0.001$, paired *t*-test). Thus, the integration of vestibular and proprioceptive inputs cannot account for the suppression of VO neuronal responses during active motion.

We next performed the same analysis on our population of V + N neurons. Figure 4*B* (left panel) depicts response vectors for each V + N neuron during passive vestibular (purple arrows) versus passive proprioceptive stimulation (green arrows). On average, V + N neurons were ~50% more sensitive to vestibular stimulation [0.35 ± 0.13 (spk/s)/(°/s)] than proprioceptive stimulation [0.26 ± 0.10 (spk/s)/(°/s); $n = 22$, $P = 0.02$, paired t-test], and responses to each modality were opposite in phase.

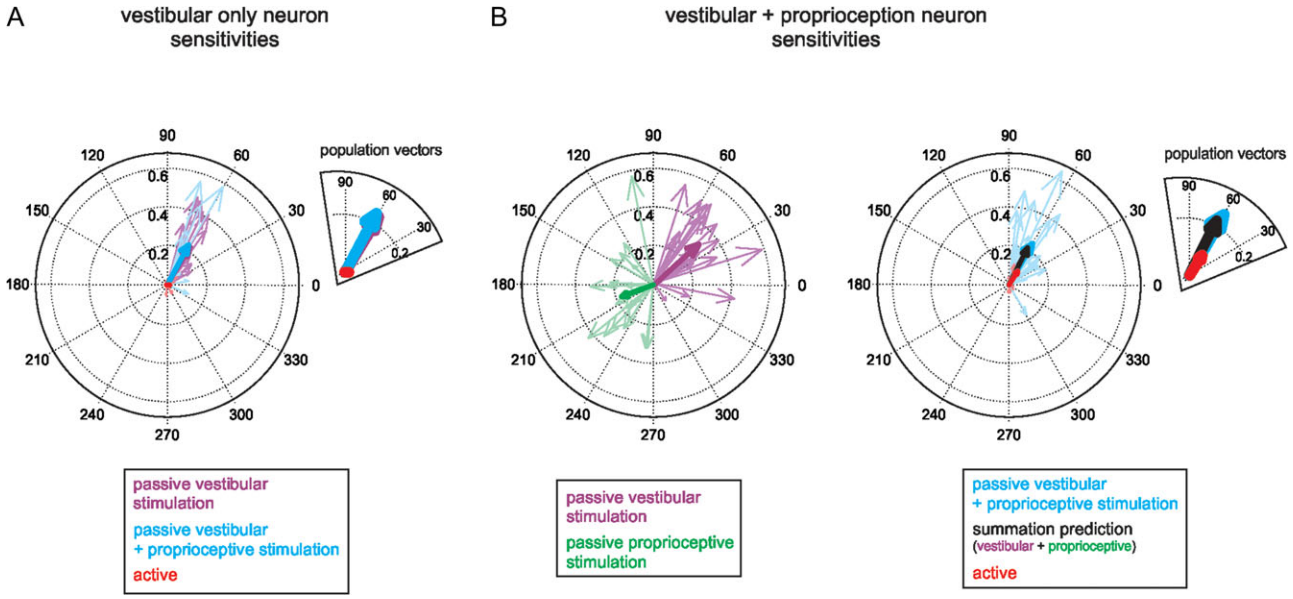

Figure 4. Integration of vestibular and neck proprioceptive inputs. (*A*) Polar plots representing the sensitivity and phase of VO neuronal responses to passive vestibular stimulation alone (purple) or combined vestibular and neck proprioceptive stimulation (passive: blue; active: red). Heavy arrows are population mean vectors. Inset shows magnified view. (*B*) Polar plots representing the sensitivity and phase of V + N neuronal responses to isolated passive vestibular (purple) or passive neck proprioceptive (green) stimulation (left panel) or to combined vestibular and neck proprioceptive stimulation (right panel; passive: blue; active: red). Heavy arrows are population mean vectors. The superimposed black arrow (see inset for magnified view) represents the population mean vector predicted from neuron-by-neuron vector summation of vestibular and neck proprioceptive sensitivities.

To then determine how V + N neurons integrate their vestibular and neck proprioceptive inputs, we quantified their responses to combined passive stimulation (Fig. 4*B*, right panel; blue arrows). We next compared this response with the linear sum of each neuron's response to passive vestibular and proprioceptive stimulation when each was applied alone (average summation prediction 0.23 ± 0.14 [spk/s]/[°/s]). Notably, on average the measured response to combined passive stimulation and the summation prediction were well matched (Fig. 4*B*, thick blue and black arrows, respectively; $n = 22$, $P = 0.39$, paired *t*-test). Furthermore, the summation prediction greatly overestimated V + N neuronal responses to active head-on-body motion (Fig. 4*B*, red arrows; $n = 22$ $P < 10^{-4}$, paired *t*-test). Thus, together these findings establish that the responses of both VO and V + N neurons during passive head-on-body rotations can be predicted by the linear summation of their vestibular and proprioceptive sensitivities, and demonstrate that the integration of vestibular and proprioceptive inputs itself does not contribute to attenuating responses to these sensory-related inputs during active movements.

VPL Neuronal Responses are not Canceled by a Motor Efference Copy

A second possibility is that a copy of the motor command to the neck musculature to move the head (e.g., efference copy signal) provides direct inhibitory inputs to VPL neurons that suppress responses during active head rotations. To test whether this mechanism contributed to selective elimination of vestibular sensitivity to active head-on-body rotations, we measured neuronal responses while monkeys attempted to make gaze shifts between 2 targets but their heads were restrained (Fig. 5). Monkeys produced large neck torques (2.9 ± 1.1 N m; upper inset of Fig. 5), signifying the generation of motor commands comparable to those generated during active movements (Roy and Cullen 2004). However, although monkeys generated motor commands to move their necks, VPL neuronal firing rates did not change for attempted head movements in either the same (ipsi; $n = 10$ VO, $P = 0.73$, $n = 9$ V + N, $P = 0.27$, paired *t*-tests; circles) or opposite (contra; $n = 10$ VO, $P = 0.05$, $n = 9$ V + N, $P = 0.61$, paired *t*-tests; diamonds) direction as their preferred direction during passive rotations. Indeed, as summarized in the lower inset of Figure 5, neuronal firing rates of both VO (black bars) and V + N neurons (white bars) remained unchanged from baseline levels. Thus, taken together, our results do not support the hypothesis that a neck efference copy signal provides direct inhibitory inputs to VPL neurons to suppress responses to active vestibular stimulation.

VPL Neuronal Responses are Minimal During Slow Active Motion, and Active Translations

Finally, to test the generalizability of our findings so far, we asked whether VPL neurons also demonstrated similar attenuation during other types of active head movement. Specifically, we focused on active head rotations that were slower than those produced during large eye-head gaze shifts (i.e., Fig. 6*A*, *B*), as well as active head translations (Fig. 6*C*).

First, we tested whether or not the same cancellation signal responsible for the selective encoding of passive head rotations during rapid gaze shifts achieved comparable attenuation of neuronal responses to slow active movements (eye/head gaze pursuit, peak velocity ~40 °/s, 0.5 and 1 Hz). Figure 6*A* shows the responses of example VO (top panel) and V + N (bottom panel) neurons during slow passive (left side, blue traces) as compared with slow active (right side, red traces) movements. In agreement with the results above (Fig. 1), both example neurons demonstrated robust responses in the passive condition (blue traces; population average sensitivities 0.61 ± 0.30 [spk/s]/[°/s] and 0.50 ± 0.18 [spk/s]/[°/s] for VO and V + N neurons,

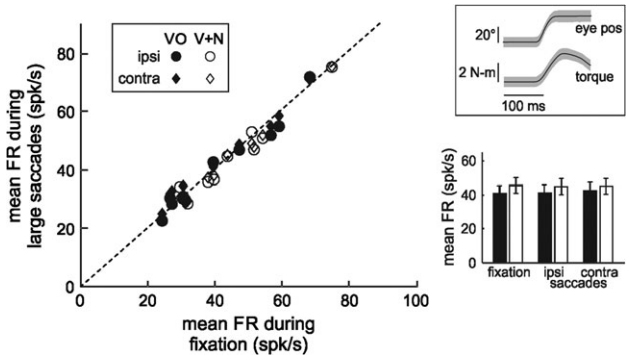

Figure 5. Neuronal activity during motor inputs. Scatter plot depicts mean neuronal firing rates during large saccades that produce neck torque in the same (ipsi, circles) or opposite (contra, diamonds) direction to the neuron's preferred direction of rotation compared with mean neuronal firing rates during eye/head fixation (VO ipsi: $n = 10$, $P = 0.73$; VO contra: $n = 10$, $P = 0.05$; V + N ipsi: $n = 9$, $P = 0.27$; V + N contra: $n = 9$, $P = 0.61$, paired *t*-tests). *Top inset*: average magnitude eye position and neck torque traces for 10 example movements. Shading shows standard deviation. *Bottom inset*: population average firing rates during fixations or saccades with torque in the ipsilateral or contralateral direction. Black and white symbols represent VO and V + N neurons, respectively.

respectively). Notably, during passive motion, neurons were more sensitive to slower head rotations than fast rotations (Fig. 6*B*, dark bars), consistent with prior characterizations of VPL neurons in squirrel monkey (Marlinski and McCrea 2008a). Sensitivities increased by ~130% ($n = 13$, $P = 0.0003$, paired *t*-test) and ~70% ($n = 23$, $P = 0.0009$, paired *t*-test) for VO and V + N neurons, respectively. Despite greater vestibular sensitivities to slow passive movements, however, both example neurons exhibited minimal firing rate modulation during active slow gaze pursuit (Fig. 6*A*, red traces). Overall, VO and V + N neuronal sensitivities were reduced 92 ± 17% ($n = 13$ VO, $P < 10^{-5}$, paired *t*-test) and 93 ± 13% ($n = 23$ V + N, $P < 10^{-11}$, paired *t*-test), respectively, relative to comparable passive head motion. Figure 6*B* summarizes our results, namely that while both groups of VPL neurons exhibit increased sensitivity for decreasing rotational velocities, neuronal response sensitivities were indeed similarly and substantially reduced to the same low levels for both slow and fast active rotations (Fig. 6*B*, compare dark and light bars).

We next addressed whether the responses of VPL neurons were likewise substantially attenuated during active translational head movements, during which the vestibular input is driven by signals from the otolith organs instead of the semicircular canals. Twenty-nine neurons in our population responded to passive whole-body translations in addition to rotations in a manner consistent with prior characterizations of VPL neuron responses (Meng et al. 2007; Meng and Angelaki 2010). Here, we were able to maintain isolation of a subset of these neurons ($n = 7$) to test the hypothesis that they would preferentially encode passive, but not active, linear motion. Figure 6*C* illustrates the responses of example VO (top panel) and V + N neurons (bottom panel). In agreement with our hypothesis, each neuron responded robustly to passively applied translations (left column, blue traces), but exhibited substantially reduced modulation in response to comparable active translations (right column, red traces). The examples shown were typical of our sample (average passive sensitivity across neurons 147 ± 53 [spk/s]/*g*); overall, responses to voluntary translations were attenuated 83 ± 17% relative to passive motion ($n = 7$, $P = 0.0004$, paired *t*-test). Taken together, our results demonstrate that both VO and V + N neurons in VPL differentiate active from passive vestibular stimulation during everyday behaviors, including slow and fast rotations, translations, and concurrent passive and active self-motion.

Discussion

Our main finding is that the posterior thalamocortical vestibular pathway distinguishes active from passively applied movement in primates. Notably, we show for the first time that vestibular neurons in the VPL thalamus selectively encode passive self-motion, even when experienced concurrently with active self-motion. Further, the responses of the individual neurons were markedly (~80%) suppressed during both active rotations and translations. This was true for neurons that were sensitive to passive stimulation of both the vestibular and proprioceptive systems, as well as for neurons sensitive only to passive vestibular stimulation. We examined the mechanism underlying the dramatic reduction of neuronal responses to active movements and found that neither the generation of a motor command (e.g., efference copy signal) nor activation of proprioceptors alone could explain the observed suppression. Taken together, our findings indicate that thalamic inputs to cortex encode vestibular sensory information in a manner that depends on whether the sensory stimulation was self-generated or externally applied. Specifically, self-motion signals arising from active head movements are canceled, such that self-motion information resulting from unexpected (i.e., passive) stimulation is preferentially conveyed to cortical processing centers by the posterior thalamus. Our results thus provide new insight into how the brain ensures stable perception during natural behaviors, by establishing that sensory inputs to cortical centers account for the sensory consequences of voluntary behavior.

Cancellation of VPL Responses to Active Self-Motion: Mechanisms

Our present results provide the first direct demonstration that the responses of neurons in the VPL thalamus selectively encode passively applied self-motion. We note that a previous study in squirrel monkeys assessed the responses of neurons in this same area, but reached the opposite conclusion that neurons respond equally well in both conditions (Marlinski and McCrea 2008b). However, there are 2 important issues that limit the interpretation of the findings of this prior study. First, neuronal sensitivities to active self-motion were never objectively quantified. In contrast, here we explicitly computed neuronal sensitivities to both active and passive self-motion to directly establish that the responses of individual neurons in this region of the thalamus are in fact markedly reduced during active as compared with passive self-motion. A second limitation of the Marlinski and McCrea study was that they did not control for the effects of visual stimulation, which could potentially augment or counteract some thalamic neurons' sensitivities to vestibular stimulation. Here, we designed our study to understand how vestibular sensory information is relayed to cortex during behavioral conditions in the absence of full-field visual stimulation. We further consider the role and potential influence of visual optic flow cues on neuronal responses below.

In 1950, von Holst and Mittelstaedt (1950) proposed an explanation for how the nervous system distinguishes between sensory inputs that are the result of external sources versus

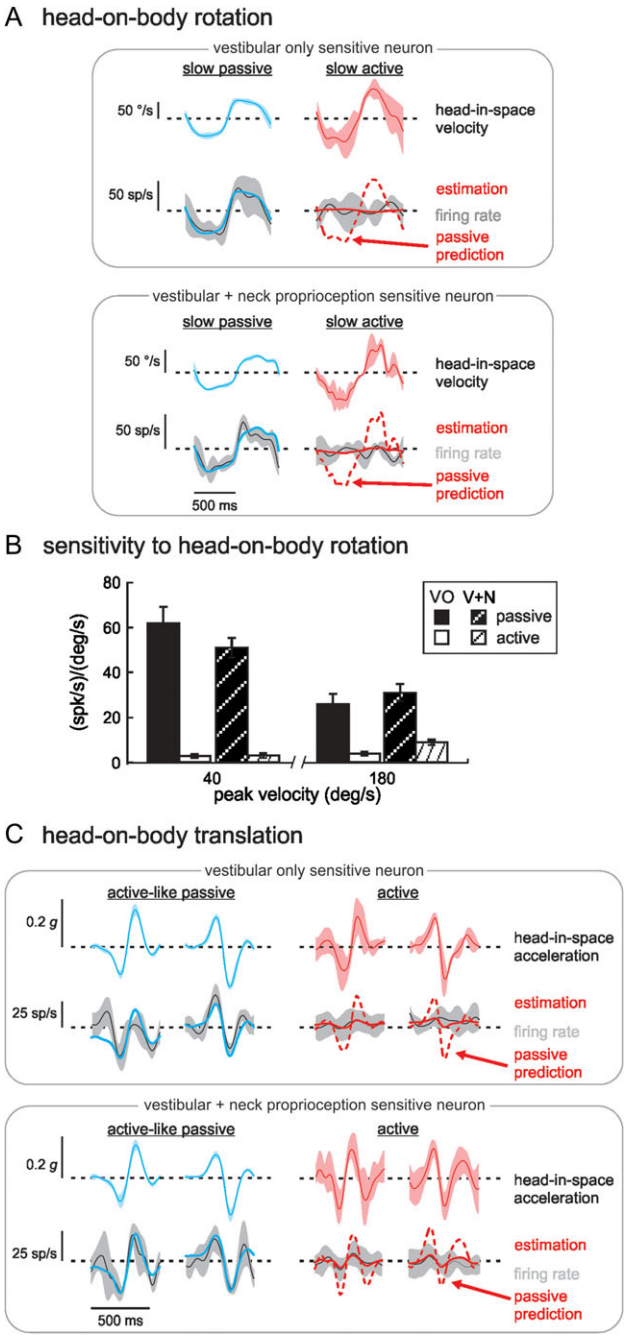

Figure 6. Neurons in the posterior vestibular thalamus selectively encode passive self-motion during slow movements and translations. (*A*) Responses of an example VO neuron (top panel) and an example V + N neuron (bottom panel) during passive (blue curves) and active (red curves) head-on-body rotations with low peak velocity. Head-in-space velocity traces represent average and standard deviation from at least 5 movements, and are plotted with the same conventions as in Figure 1. Firing rate estimations (solid blue and red curves) are based on fits to eq. 1, and passive predictions (dashed red curves) are based on sensitivity computed from the passive estimation. Conventions as in Figure 1. (*B*) Population summary. Neuronal sensitivities to fast passive motion are about half those to slow passive motion (compare black bars for 180 vs. 40 °/s; $n = 13$ VO, $P = 0.0003$, $n = 23$ V + N, $P = 0.0009$, paired *t*-tests), but in both conditions, sensitivities to active motion were reduced to similar low levels (compare white and black bars; $n = 13$ VO, $P < 10^{-5}$, $n = 23$ V + N, $P < 10^{-11}$, paired *t*-tests). (*C*) Responses of an example VO neuron (top panel) and an example V + N neuron (bottom panel) to passively applied (blue curves) and self-generated (red curves) head-on-body linear motion with comparable trajectories. Head-in-space acceleration traces show the average and standard deviation from at least 5 movements. Firing rate estimations (solid blue and red curves) represent best fits to eq. 1. Responses to active translations (red curves) are overestimated by the passive prediction (dashed red curves). Conventions: Upward is rightward (shown on the lateral/interaural axis) for all translational movement traces, and superimposed dashed lines represent 0 *g*. Light dashed lines superposed on unit firing rate traces represent the mean response.

those resulting from actively generated movement. Specifically, they proposed the "principle of reafference" which states that, in order to create a stable perception of the outside world (termed exafference), the brain computes the expected sensory consequence of an action (corollary discharge; Sperry 1950) based on a copy of the motor command (efference copy), which it then subtracts from the actual sensory signal (termed reafference; reviewed in Cullen 2011, 2012). Thus, when sensory stimulation is self-generated, this comparison effectively cancels the incoming sensory input. von Holst's and Mittelstaedt's initial proposal was furthered by behavioral and theoretical investigations (Wolpert et al. 1995; Decety 1996; Farrer et al. 2003) which suggested that sensory reafference is compared with an internal model that computes the expected sensory consequence of our behaviors. Moreover, experiments in model systems including the electrosensory systems of mormyrid fish and elasmobranches, as well as the mechanosensory system of the crayfish and the auditory system of the cricket, have provided evidence that such a comparison is made (reviewed in Cullen 2004).

At first glance, our present findings may also appear to provide support for von Holst and Mittelstaedt's "principle of reafference" (von Holst and Mittelstaedt 1950), yet there is a key difference. Specifically, the principle of reafference predicts that the brain will suppress the predicted response to self-produced stimulation, regardless of whether the behavior is enacted or prevented. Indeed, this result has been reported, for example, in the mormyrid fish electrosensory system. In this system, the brain computes a negative image of the organism's predicted reafference, whether or not the fish actually emits an electric organ discharge (Bell 1981; Sawtell et al. 2007; Requarth and Sawtell 2011). In contrast, here we established that reafference is canceled during normal active movements (i.e., Figs 2, 3, and 6), however, we never observed a negative image when head movement was prevented (i.e., Fig. 5). Thus, this difference from von Holst's and Mittelstaedt's principle of reafference suggests that the cancellation of responses to self-produced stimulation in the primate vestibular system is instead gated in a behaviorally dependent manner. Notably, a cancellation signal is only present during behavioral conditions where the actual sensory feedback from neck proprioceptors matches the brain's estimate of the sensory consequence of a voluntary movement (Fig. 7A).

While the source of the cancellation signal responsible for response suppression remains unknown, 2 possibilities have been proposed. First, Marlinski and McCrea (Marlinski and McCrea 2008b) suggested that VPL could receive an inhibitory motor efference copy, since motor related areas of cortex project to the VPL (Ipekchyan and Badalyan 2016; reviewed in: Lopez and Blanke 2011). However, as noted above, our finding that neuronal responses are not modulated in conditions where a motor command is generated but motion is prevented (i.e., Fig. 5) provides direct evidence against this proposal. A second, more likely possibility is that the mechanism responsible for the suppression of self-generated reafference involves an internal model that computes the expected sensory consequences of an action, which are then compared with the actual sensory input (Fig 7A; reviewed in: Cullen 2011, 2012). Such a mechanism is thought to underlie the cancellation of responses

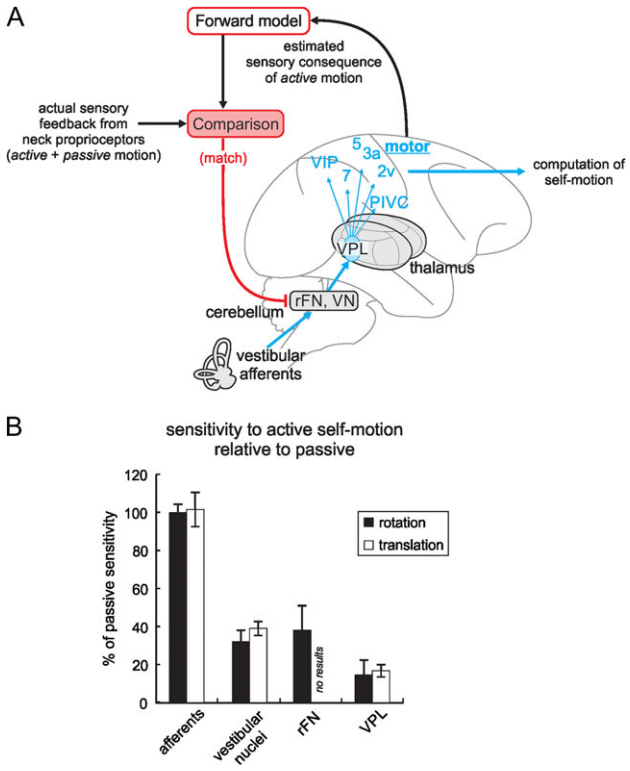

Figure 7. Proposed mechanism of attenuation of responses to voluntary movements in the posterior ascending vestibular pathway. (*A*) A comparison is made—likely in the cerebellum—between an internal model's motor command-based estimate of a self-generated head movement and the actual sensory feedback from neck proprioceptors. When there is a match, responses in early central stages of vestibular processing are inhibited (red projection), which reduces responses of thalamic neurons projecting to cortex for the computation of self-motion. Accordingly, in order to compute an estimate of active motion, cortical areas need to integrate information from multiple modalities. Areas 2 v, 3a, 5, and 7 of cortex; rFN, rostral fastigial nucleus; PIVC, parietoinsular vestibular cortex; VIP, ventral intraparietal cortex; VN, vestibular nuclei. (*B*) Population summary comparing sensitivity to active rotations (black bars) and translations (white bars) normalized relative to passive responses for 4 stages of vestibular processing (afferents: Sadeghi et al. 2007; Jamali et al. 2009; vestibular nuclei: Roy and Cullen 2001; Carriot et al. 2013; rFN: Brooks and Cullen 2013). Error bars show standard error of the mean.

to active self-motion at the level of the vestibular nuclei (Roy and Cullen 2001, 2004; Carriot et al. 2013; Brooks and Cullen 2014) as well as rostral fastigial nucleus of the cerebellum (rFN; Brooks and Cullen 2013, Cullen and Brooks 2014).

This differential processing of active versus passive head movements has important implications for voluntary motor control versus balance. For example, VO neurons in the vestibular nuclei and rFN mediate vestibulo-spinal reflexes to compensate for unexpected movements. However, during active movements these same stabilizing reflexes would be counterproductive. Accordingly, suppressing the modulation of neurons in vestibulo-spinal reflex pathways is functionally advantageous during active movements. We speculate that the computation of the expected sensory consequences of voluntary movements occurs in cerebellar cortex, which projects directly to the vestibular nuclei and rFN (Cullen and Brooks 2014; Brooks et al. 2015). The VPL, in turn, receives projections from both the vestibular nuclei (Deecke et al. 1977) and the rFN (Batton et al. 1977). Thus, we hypothesize that the mechanism underlying response cancellation in VPL is also cerebellar in origin. Moreover, as further discussed below, our findings suggest that differential processing of active versus passive head movements also has important implications for the computation of self-motion since VO neurons are the likely source of input to the VPL.

Selective Encoding of Passive Self-Motion: Implications for Perception and Behavior

The brain's ability to distinguish between sensory stimulation resulting from externally generated versus self-generated motion is vital for stable perception and accurate motor control. Here, by quantifying individual responses in VPL, we have established that neurons in posterior thalamocortical vestibular pathways selectively encode externally applied vestibular information. Our studies focused on horizontal, yaw rotations as well as translations in the horizontal plane, and we speculate that our findings will extend to coding of vestibular information for refining self-motion perception in other dimensions. For example, a recent report found that patients with strokes affecting the ventral posterior thalamus have difficulties in tasks requiring alignment with Earth vertical, consistent with significant deficits in gravity perception (Baier et al. 2016). Interestingly, Meng et al. (2007) found that during passive tilts, VPL neurons display a continuum of responses from "afferent-like" encoding of gravity to modulation only in response to the translational component of tilts. Additional studies will be required to determine whether thalamic neurons projecting to cortex continue to respond to voluntary changes in head orientation relative to gravity. Further, infarctions of the ventrolateral thalamus not only lead to abnormal processing of vestibular inputs (i.e., circling to the ipsilateral side), but also significant proprioceptive deficits on the contralateral side (Gonçalves et al. 2011). Thus, we speculate based on this and our current findings that the behaviorally dependent encoding of proprioceptive information within these pathways also plays an important role in mediating stable perception during active self-motion.

We note that our goal in the present study was to establish how vestibular sensory information is relayed to cortex during a variety of behavioral contexts (passive motion, active motion, or concurrent passive and active motion), in conditions that did not provide visual stimulation. In everyday life, however, our perception of self-motion depends on the integration of visual with vestibular and proprioceptive information. Indeed, full-field motion (optic flow) alone can produce sensations of displacement (Gibson 1950), and single unit recording experiments in the vestibular nuclei (Waespe and Henn 1977) and VPL (Büttner and Henn 1976) initially suggested that visual–vestibular integration occurs early in vestibular processing. However, as noted above non-eye movement related neurons in the vestibular nuclei (i.e., VO neurons) are the likely input to the VPL (reviewed in: Cullen 2016), and more recent studies have established that VO neurons are not reliably driven by optic flow stimuli either in the vestibular nuclei (Beraneck and Cullen 2007; Bryan and Angelaki 2009) or in the VPL (Magnin and Fuchs 1977; Meng et al. 2007). Understanding the source of the discrepancy between these previous studies, as well as how VPL neurons integrate vestibular, proprioceptive, and motor information with optic flow information during active self-motion will be an important direction for future work.

Cortical Targets of VPL Neurons: The Differential Transmission of Vestibular Information

Imaging and electrophysiological studies have established that projections from VPL activate cortical targets, most notably the

parietoinsular vestibular cortex (PIVC; Dieterich et al. 2005) and ventral intraparietal cortex (VIP; Matsuzaki et al. 2004). In turn, there is evidence to support a role for both of these areas in self-motion perception. First, PIVC stimulation produces a sensation of turning as well as dizziness (Penfield 1957), and PIVC inactivation impairs vestibular perceptual thresholds (Chen et al. 2016). Second, VIP neuronal responses are highly correlated with monkeys' behavioral responses during vestibular heading discrimination (Chen et al. 2013). Surprisingly, a recent study concluded that inactivation of VIP does not affect vestibular perceptual thresholds (Chen et al. 2016). However, this study did not test monkeys' responses in the absence of a visual stimulus either producing optic flow or activating the pursuit pathway. This leaves the possibility that VIP neurons are causally involved in perception of purely vestibular stimuli unaddressed. Importantly, areas PIVC and VIP both also encode numerous other sensory signals (e.g., proprioceptive, somatosensory, and visual) in addition to vestibular information (PIVC: Akbarian et al. 1988; Grüsser et al. 1990a, b; Akbarian et al. 1992; Chen et al. 2010; and VIP: Bremmer et al. 2002; Schlack et al. 2002; Chen et al. 2011; reviewed in: Britten 2008). As such, VPL is likely a key source of multisensory input to these cortical regions, and our present results reveal that VPL neuronal responses to vestibular and proprioceptive stimulation during voluntary movements are suppressed across a wide range of self-motion behaviors. Notably, we found comparable suppression for active rapid gaze shifts and slower gaze pursuit (Fig. 6*B*), as well as for both rotations and translations (Fig. 7*B*). Thus, the suppression of these self-motion signals was robust across all active behaviors that we tested.

Finally, our present results identify a clear trend across subsequent stages of ascending vestibular pathways. As shown in Figure 7*B*, while primary vestibular afferents show no response attenuation during active motion (Sadeghi et al. 2007; Jamali et al. 2009), neurons at each subsequent stage of central processing are increasingly selective to passive self-motion. As discussed above, it is currently understood that during passive stimulation, vestibular sensory information is combined with visual and somatosensory cues to provide an estimate of self-motion in a network of cortical areas involved in perception. Importantly, however, the cortical processing of active self-motion has not been widely studied. Indeed, to date, a single study has compared the responses of neurons in PIVC during passive and active gaze shifts (Shinder and Newlands 2014). While the authors reported no difference in the 2 conditions, they emphasized that PIVC neurons appear to encode differences in self-motion relative to objects in the environment and that this likely biased their results. Correspondingly, to date, a single study has compared the responses of neurons in area VIP to passive and active self-motion (Klam and Graf 2006). Consistent with our proposal, neuronal signals were most often seen to be diminished in the active movement condition compared with passive stimulation. Future experiments will be necessary to fully understand how these cortical areas integrate inputs from VPL with vestibular information from other parts of the brain to encode self-motion during voluntary, task-dependent behaviors.

Conclusion

In summary, we show for the first time that neurons in the posterior thalamus robustly encode sensory signals during passively applied self-motion, but that neuronal responses to vestibular and proprioceptive stimulation resulting from active movement are markedly suppressed. Accordingly, our findings reveal a novel feature of sensory coding by thalamocortical pathways, namely that the VPL thalamus preferentially encodes externally applied versus active movement. We speculate that this differential transmission of sensory information to cortex is vital for ensuring stable perception during motion as well as accurate motor control during everyday activities.

Funding

The National Institute on Deafness and Other Communication Disorders at the National Institutes of Health (grants R01-DC002390, R01-DC009255, and R01-DC013069 to K.E.C.) and the Canadian Institutes of Health Research.

Notes

We thank J.X. Brooks, O. Zobeiri, D. Mitchell, K. Dyson, I. Mackrous, N. Bent, and X.S. Hu for feedback on the manuscript. Dr. Ninglei Sun contributed to data collection for monkey S. Walter Kucharski and Stephen Nuara provided crucial technical assistance. *Conflict of interest*: The authors declare no competing financial interests.

References

Akbarian S, Berndl K, Grüsser OJ, Guldin W, Pause M, Schreiter U. 1988. Responses of single neurons in the parietoinsular vestibular cortex of primates. Ann N Y Acad Sci. 545:187–202.

Akbarian S, Grüsser OJ, Guldin WO. 1992. Thalamic connections of the vestibular cortical fields in the squirrel monkey (*Saimiri sciureus*). J Comp Neurol. 326(3):423–441.

Baier B, Conrad J, Stephan T, Kirsch V, Vogt T, Wilting J, Muller-Forell W, Dieterich M. 2016. Vestibular thalamus: two distinct graviceptive pathways. Neurology. 86(2):134–140.

Batton RR 3rd, Jayaraman A, Ruggiero D, Carpenter MB. 1977. Fastigial efferent projections in the monkey: an autoradiographic study. J Comp Neurol. 174(2):281–305.

Bell CC. 1981. An efference copy which is modified by reafferent input. Science. 214(4519):450–453.

Beraneck M, Cullen KE. 2007. Activity of vestibular nuclei neurons during vestibular and optokinetic stimulation in the alert mouse. J Neurophysiol. 98(3):1549–1565.

Bremmer F, Klam F, Duhamel JR, Ben Hamed S, Graf W. 2002. Visual-vestibular interactive responses in the macaque ventral intraparietal area (VIP). Eur J Neurosci. 16(8):1569–1586.

Britten KH. 2008. Mechanisms of self-motion perception. Annu Rev Neurosci. 31:389–410.

Brooks JX, Carriot J, Cullen KE. 2015. Learning to expect the unexpected: rapid updating in primate cerebellum during voluntary self-motion. Nat Neurosci. 18(9):1310–1317.

Brooks JX, Cullen KE. 2009. Multimodal integration in rostral fastigial nucleus provides an estimate of body movement. J Neurosci. 29(34):10499–10511.

Brooks JX, Cullen KE. 2013. The primate cerebellum selectively encodes unexpected self-motion. Curr Biol. 23(11):947–955.

Brooks JX, Cullen KE. 2014. Early vestibular processing does not discriminate active from passive self-motion if there is a discrepancy between predicted and actual proprioceptive feedback. J Neurophysiol. 111(12):2465–2478.

Bryan AS, Angelaki DE. 2009. Optokinetic and vestibular responsiveness in the macaque rostral vestibular and fastigial nuclei. J Neurophysiol. 101(2):714–720.

Büttner U, Buettner UW. 1978. Parietal cortex (2v) neuronal activity in the alert monkey during natural vestibular and optokinetic stimulation. Brain Res. 153(2):392–397.

Büttner U, Henn V. 1976. Thalamic unit activity in the alert monkey during natural vestibular stimulation. Brain Res. 103(1):127–132.

Büttner U, Lang W. 1979. The vestibulocortical pathway: neurophysiological and anatomical studies in the monkey. Prog Brain Res. 50:581–588.

Carriot J, Brooks JX, Cullen KE. 2013. Multimodal integration of self-motion cues in the vestibular system: active versus passive translations. J Neurosci. 33(50):19555–19566.

Carriot J, Jamali M, Brooks JX, Cullen KE. 2015. Integration of canal and otolith inputs by central vestibular neurons is subadditive for both active and passive self-motion: implication for perception. J Neurosci. 35(8):3555–3565.

Chen A, DeAngelis GC, Angelaki DE. 2010. Macaque parieto-insular vestibular cortex: responses to self-motion and optic flow. J Neurosci. 30(8):3022–3042.

Chen A, DeAngelis GC, Angelaki DE. 2011. Representation of vestibular and visual cues to self-motion in ventral intraparietal cortex. J Neurosci. 31(33):12036–12052.

Chen A, Deangelis GC, Angelaki DE. 2013. Functional specializations of the ventral intraparietal area for multisensory heading discrimination. J Neurosci. 33(8):3567–3581.

Chen A, Gu Y, Liu S, DeAngelis GC, Angelaki DE. 2016. Evidence for a causal contribution of macaque vestibular, but not intraparietal, cortex to heading perception. J Neurosci. 36 (13):3789–3798.

Cherif S, Cullen KE, Galiana HL. 2008. An improved method for the estimation of firing rate dynamics using an optimal digital filter. J Neurosci Methods. 173(1):165–181.

Clark BJ, Harvey RE. 2016. Do the anterior and lateral thalamic nuclei make distinct contributions to spatial representation and memory? Neurobiol Learn Mem. 133:69–78.

Cullen KE. 2004. Sensory signals during active versus passive movement. Curr Opin Neurobiol. 14(6):698–706.

Cullen KE. 2011. The neural encoding of self-motion. Curr Opin Neurobiol. 21(4):587–595.

Cullen KE. 2012. The vestibular system: multimodal integration and encoding of self-motion for motor control. Trends Neurosci. 35(3):185–196.

Cullen KE. 2016. Physiology of central pathways. Handb Clin Neurol. 137:17–40.

Cullen KE, Brooks JX. 2014. Neural correlates of sensory prediction errors in monkeys: evidence for internal models of voluntary self-motion in the cerebellum. Cerebellum. 14(1):31–34.

Cullen KE, Roy JE. 2004. Signal processing in the vestibular system during active versus passive head movements. J Neurophysiol. 91(5):1919–1933.

Dale A, Cullen KE. 2013. The nucleus prepositus predominantly outputs eye movement-related information during passive and active self-motion. J Neurophysiol. 109(7):1900–1911.

Dale A, Cullen KE. 2015. Local population synchrony and the encoding of eye position in the primate neural integrator. J Neurosci. 35(10):4287–4295.

Decety J. 1996. Neural representations for action. Rev Neurosci. 7(4):285–297.

Deecke L, Schwarz DW, Fredrickson JM. 1977. Vestibular responses in the rhesus monkey ventroposterior thalamus. II. Vestibulo-proprioceptive convergence at thalamic neurons. Exp Brain Res. 30(2–3):219–232.

Dieterich M, Bartenstein P, Spiegel S, Bense S, Schwaiger M, Brandt T. 2005. Thalamic infarctions cause side-specific suppression of vestibular cortex activations. Brain. 128(Pt 9): 2052–2067.

Duensing F, Schaefer KP. 1958. [The activity of single neurons in the region of vestibular nuclei in horizontal acceleration, with special reference to vestibular nystagmus]. Arch Psychiatr Nervenkr Z Gesamte Neurol Psychiatr. 198: 225–252.

Duffy CJ. 1998. MST neurons respond to optic flow and translational movement. J Neurophysiol. 80(4):1816–1827.

Dumont JR, Taube JS. 2015. The neural correlates of navigation beyond the hippocampus. Prog Brain Res. 219:83–102.

Farrer C, Franck N, Paillard J, Jeannerod M. 2003. The role of proprioception in action recognition. Conscious Cogn. 12(4): 609–619.

Fuchs AF, Robinson DA. 1966. A method for measuring horizontal and vertical eye movement chronically in the monkey. J Appl Physiol. 21(3):1068–1070.

Gibson JJ. 1950. The perception of visual surfaces. Am J Psychol. 63(3):367–384.

Gonçalves R, Carrera I, Garosi L, Smith PM, Fraser McConnell J, Penderis J. 2011. Clinical and topographic magnetic resonance imaging characteristics of suspected thalamic infarcts in 16 dogs. Vet J. 188(1):39–43.

Grüsser OJ, Pause M, Schreiter U. 1990a. Localization and responses of neurones in the parieto-insular vestibular cortex of awake monkeys (*Macaca fascicularis*). J Physiol. 430: 537–557.

Grüsser OJ, Pause M, Schreiter U. 1990b. Vestibular neurones in the parieto-insular cortex of monkeys (*Macaca fascicularis*): visual and neck receptor responses. J Physiol. 430:559–583.

Hayes AV, Richmond BJ, Optican LM. 1982. A UNIX-based multiple process system for real-time data acquisition and control. WESCON Conf Proc. 2:1–10.

Hitier M, Besnard S, Smith PF. 2014. Vestibular pathways involved in cognition. Front Integr Neurosci. 8:59.

Ipekchyan NM, Badalyan SA. 2016. [The distribution of cortico-thalamic projections of different of different somatotopic representations of primary motor and sensory cortex]. Morfologiia. 149(1):15–21.

Jamali M, Sadeghi SG, Cullen KE. 2009. Response of vestibular nerve afferents innervating utricle and saccule during passive and active translations. J Neurophysiol. 101(1):141–149.

Judge SJ, Richmond BJ, Chu FC. 1980. Implantation of magnetic search coils for measurement of eye position: an improved method. Vision Res. 20(6):535–538.

Klam F, Graf W. 2006. Discrimination between active and passive head movements by macaque ventral and medial intraparietal cortex neurons. J Physiol. 574(Pt 2):367–386.

Laurens J, Kim B, Dickman JD, Angelaki DE. 2016. Gravity orientation tuning in macaque anterior thalamus. Nat Neurosci. 19(12):1566–1568.

Lopez C, Blanke O. 2011. The thalamocortical vestibular system in animals and humans. Brain Res Rev. 67(1-2):119–146.

Magnin M, Fuchs AF. 1977. Discharge properties of neurons in the monkey thalamus tested with angular acceleration, eye movement and visual stimuli. Exp Brain Res. 28(3-4): 293–299.

Marlinski V, McCrea RA. 2008a. Activity of ventroposterior thalamus neurons during rotation and translation in the horizontal plane in the alert squirrel monkey. J Neurophysiol. 99 (5):2533–2545.

Marlinski V, McCrea RA. 2008b. Coding of self-motion signals in ventro-posterior thalamus neurons in the alert squirrel monkey. Exp Brain Res. 189(4):463–472.

Marrocco RT. 1976. Sustained and transient cells in monkey lateral geniculate nucleus: conduction velocites and response properties. J Neurophysiol. 39(2):340–353.

Matsuzaki R, Kyuhou S, Matsuura-Nakao K, Gemba H. 2004. Thalamo-cortical projections to the posterior parietal cortex in the monkey. Neurosci Lett. 355(1-2):113–116.

Meng H, Angelaki DE. 2010. Responses of ventral posterior thalamus neurons to three-dimensional vestibular and optic flow stimulation. J Neurophysiol. 103(2):817–826.

Meng H, May PJ, Dickman JD, Angelaki DE. 2007. Vestibular signals in primate thalamus: properties and origins. J Neurosci. 27(50):13590–13602.

Moser EI, Kropff E, Moser MB. 2008. Place cells, grid cells, and the brain's spatial representation system. Annu Rev Neurosci. 31: 69–89.

Penfield W. 1957. Vestibular sensation and the cerebral cortex. Ann Otol Rhinol Laryngol. 66(3):691–698.

Requarth T, Sawtell NB. 2011. Neural mechanisms for filtering self-generated sensory signals in cerebellum-like circuits. Curr Opin Neurobiol. 21(4):602–608.

Robertson RG, Rolls ET, Georges-Francois P, Panzeri S. 1999. Head direction cells in the primate pre-subiculum. Hippocampus. 9 (3):206–219.

Roy JE, Cullen KE. 2001. Selective processing of vestibular reafference during self-generated head motion. J Neurosci. 21(6): 2131–2142.

Roy JE, Cullen KE. 2004. Dissociating self-generated from passively applied head motion: neural mechanisms in the vestibular nuclei. J Neurosci. 24(9):2102–2111.

Sadeghi SG, Minor LB, Cullen KE. 2007. Response of vestibular-nerve afferents to active and passive rotations under normal conditions and after unilateral labyrinthectomy. J Neurophysiol. 97(2): 1503–1514.

Sadeghi SG, Mitchell DE, Cullen KE. 2009. Different neural strategies for multimodal integration: comparison of two macaque monkey species. Exp Brain Res. 195(1):45–57.

Sakata H, Shibutani H, Ito Y, Tsurugai K, Mine S, Kusunoki M. 1994. Functional properties of rotation-sensitive neurons in the posterior parietal association cortex of the monkey. Exp Brain Res. 101(2):183–202.

Sawtell NB, Williams A, Bell CC. 2007. Central control of dendritic spikes shapes the responses of Purkinje-like cells through spike timing-dependent synaptic plasticity. J Neurosci. 27(7):1552–1565.

Schlack A, Hoffmann KP, Bremmer F. 2002. Interaction of linear vestibular and visual stimulation in the macaque ventral intraparietal area (VIP). Eur J Neurosci. 16(10):1877–1886.

Shinder ME, Newlands SD. 2014. Sensory convergence in the parieto-insular vestibular cortex. J Neurophysiol. 111(12): 2445–2464.

Shinder ME, Taube JS. 2010. Differentiating ascending vestibular pathways to the cortex involved in spatial cognition. J Vestib Res. 20(1):3–23.

Sperry RW. 1950. Neural basis of the spontaneous optokinetic response produced by visual inversion. J Comp Physiol Psychol. 43:482–489.

Taube JS. 2007. The head direction signal: origins and sensory-motor integration. Annu Rev Neurosci. 30:181–207.

von Holst E, Mittelstaedt H. 1950. Das Reafferenzprinzip. Naturwissenschaften. 37:464–476.

Waespe W, Henn V. 1977. Neuronal activity in the vestibular nuclei of the alert monkey during vestibular and optokinetic stimulation. Exp Brain Res. 27(5):523–538.

Wijesinghe R, Protti DA, Camp AJ. 2015. Vestibular interactions in the thalamus. Front Neural Circuits. 9:79.

Wolpert DM, Ghahramani Z, Jordan MI. 1995. An internal model for sensorimotor integration. Science. 269(5232):1880–1882.